14th Australasian Fluid Mechanics Conference
Adelaide University, Adelaide, Australia
10-14 December 2001

Numerical Simulation of Abrasive Water Jet for Different Taper Inlet Angles

Dewan H. Ahmed[1], Elias Siores[1], Jamal Naser[2], Frank L. Chen[1]

[1]Industrial Research Institute Swinburne
Swinburne University of Technology, Hawthorn, Victoria, 3122 AUSTRALIA

[2]School of Engineering and Science
Swinburne University of Technology, Hawthorn, Victoria, 3122 AUSTRALIA

Abstract

Abrasive water jet uses for precision cutting in modern technology. A Computational Fluid Dynamics (CFD) method has been developed to find out the particle, water and air velocity distributions for abrasive water jet. The study has been carried out using a multi-phase approach. The granular abrasive particles were treated a continuous phase. The air used for pumping the abrasive particles into the jet device was treated as a continuous phase and the water was treated as the principal continuous phase. The governing equations were discretized using the finite volume approach. The solutions were obtained using the Inter-Phase Slip Algorithm (IPSA). The governing equations were closed using the k-ε turbulence model. As the jet velocity depends on the acceleration process of water and abrasive particles, the simulation was performed using different taper inlet angles. It was found from the simulations that the acceleration process was much better for higher taper inlet angle leading to the maximum velocity of the jet at the exit of the focus tube. The velocities and volume fractions of air, water and abrasive particles at the exit were compared with the available experimental data. The simulated results showed reasonably good agreement with the experimental data.

Introduction

In the early 1980s, abrasive water jet cutting system was established for it's great advantages over alternative conventional cutting processes. There are mainly two ways to add the abrasive material to the fluid: the injection system and the suspension system. The injection procedure consists of an acceleration of the pure water and a subsequent addition and acceleration of the abrasive particles. A great part of the resulting jet consists of air due its large volume fraction. In contrast to the injection jet the suspension jet has no gaseous component. The mixing of the abrasive and water happens under pressure before the acceleration process starts. Hashish [3] showed that the advantage of the suspension system is a higher effectiveness and a more coherent jet structure. This has to be paid for by the stronger erosion wear of the nozzle. Since abrasive jets are made up of three-phases, the parameters that control their properties are much more complex than that of plain water jets. During the last five years abundant number of thorough investigations have been carried out to understand the basics of the mixing process, the characteristics of the jets, and their cutting behaviour [4].

Abrasive water jets work by removing the target material mainly by impacts of abrasive material particles. The cutting performance of an abrasive water jet is a function of the total mass of impinging particles and their velocity at the impact. So the average velocity of the total mass of abrasive particles is a quantity which must be well determined to improve the cutting head design. Abrasive water jet is used for the precision cutting in modern industries for different applications. The high-pressure water is passing through the orifice and transfers the momentum to accelerate the particles. The particles are introduced through the side inlet with small velocity. For precision cutting jet velocity at the outlet is the very important. The cutting efficiency of abrasive water jet depends on several parameters: mixing chamber diameter, mixing chamber length, taper inlet angle, focus tube diameter, focus tube length, orifice diameter and also abrasive inlet angle.

Scharner [7] calculated the air flow rate according to the abrasive flow rate. It is clear from their paper that the geometry of the mixing chamber has a great influence on the air flow rate. Abduka and Crofton [1] showed that the vacuum pressure inside the mixing chamber increases with the increase of the water pressure and the orifice diameter. Neusen [6] showed that the composition of abrasive water jet on a volume basis is approximately 4% to 6% water, 0.2% to 0.5% abrasive and 93% to 95% air. Tazibt [8] showed that the air sucked in with the abrasive particles occupies more than 90 percent of the volume of an abrasive water jet slurry and hence there is a great influence of air in abrasive water jet. Some authors have tried to simulate the abrasive water jet but they have only considered two phases (water and solid). Ye J. [9] attempted to simulate the abrasive water jet considering the particle motion and trajectories with Lagrangian equations of particle motion. He showed that the tapered inlet angle has profound influence on the particle concentration and kinetic energy distribution at the nozzle exit. Ye J. and Kovacevic R. [10] have also simulated the abrasive water jet for two phases and in both the simulations they used a direct injected abrasive water jet (DIA jet). In this paper effort has been made to simulate abrasive water jet considering three phases for conventional entrainment jets.

Mathematical Modelling

Introduction

Abrasive water jet is associated with highly turbulent flow. To predict the velocity distribution at the nozzle exit, water, air and solid slurry needs to be treated as a multi-phase system. The simulations are carried out for steady state, turbulent flow with heat transfer. Water was considered as the primary phase. Simulations were made with k-ε turbulence model (turbulent kinetic energy and energy dissipation) using the CFX-4.

Equations of the Simulations

The three phases were labelled by Greek indices α, β and γ representing water, air and solid respectively and N_p denotes the number of phases. The volume fraction of each phase is denoted by r_α. Governing equations were solved for the time averaged values of the velocity components, pressure, volume fractionsand turbulence parameters. The equations were closed using k-ε turbulence model. The equations are presented below. Hence the subscript α denotes the phase water. Equations for air and solid phases can be obtained by replacing α with β and γ respectively.

The continuity equation

$$\nabla.\left(r_\alpha \rho_\alpha \mathbf{U}_\alpha\right)=0 \tag{1}$$

The momentum equation

$$\begin{aligned}&\nabla.\left(r_\alpha\left(\rho_\alpha \mathbf{U}_\alpha-\mu_{\alpha eff}\left(\nabla \mathbf{U}_\alpha+\left(\nabla \mathbf{U}_\alpha\right)^T\right)\right)\right)\\&=r_\alpha\left(\mathbf{B}-\nabla p_\alpha\right)+\sum_{\beta=1}^{N_p} c_{\alpha\beta}^{(d)}\left(\mathbf{U}_\alpha-\mathbf{U}_\beta\right)+\mathbf{F}_\alpha\end{aligned} \tag{2}$$

$c_{\alpha\beta}^{(d)}$ is the inter-phase drag term between phase α (water) and phase β (air).

Where $\mu_{\alpha eff}=\mu_\alpha+\mu_{T\alpha}$ (3)

$\mu_{\alpha eff}$ is the effective viscosity, μ_α is the molecular viscosity and $\mu_{T\alpha}$ is the turbulent viscosity.

and $\mu_{T\alpha}=C_\mu \rho_\alpha \dfrac{k_\alpha^2}{\varepsilon_\alpha}$ (4)

Here k is the turbulence kinetic energy and ε is the dissipation length scale.

The energy equation

$$\nabla.\left(r_\alpha\left(\rho_\alpha \mathbf{U}_\alpha H_\alpha-\lambda_\alpha \nabla T_\alpha\right)\right)=\sum_{\beta=1}^{N_p} c_{\alpha\beta}^{(h)}\left(T_\beta-T_\alpha\right) \tag{5}$$

where H_α is the static enthalpy, $H_\alpha=h_\alpha\left(T_\alpha\right)$

$c_{\alpha\beta}^{(h)}$ is the inter-phase heat transfer term.

So, the constitutive equation for each phase is as follows:

$$h_\alpha=h_\alpha\left(T_\alpha p_\alpha\right) \tag{6}$$

Considering that the volume fractions sum is unity:

$$\sum_{\alpha=1}^{N_p} r_\alpha=1$$

The general advection-diffusion equation is:

$$\begin{aligned}&\nabla.\left(r_\alpha\left(\rho_\alpha \mathbf{U}_\alpha \Phi_\alpha-\Gamma_\alpha \nabla \Phi_\alpha\right)\right)\\&=r_\alpha S_\alpha+\sum_{\beta=1}^{N_p} c_{\alpha\beta}\left(\Phi_\beta-\Phi_\alpha\right)\end{aligned} \tag{7}$$

Γ is the eddy diffusivity

The term $c_{\alpha\beta}\left(\Phi_\beta-\Phi_\alpha\right)$ describes inter-phase transfer of Φ between α and β.

$c_{\alpha\alpha}=0$, $c_{\alpha\beta}=c_{\beta\alpha}$. Hence, the sum over all phases of all inter-phase transfer terms is zero.

Equation of volume fraction

$$\nabla.\left(r_\alpha \rho_\alpha \mathbf{U}_\alpha-\Gamma_\alpha \nabla r_\alpha\right)=0 \tag{8}$$

where $\Gamma_\alpha=\dfrac{\mu_{T\alpha}}{\sigma_\alpha}$ and σ_α is the turbulent Prandtl number.

The turbulent dispersion of volume fraction was modelled using the Eddy diffusivity hypothesis.

The transport equation for k and ε takes the same form as the generic scalar advection-diffusion equation

$$\begin{aligned}&\nabla.\left(r_\alpha\left(\rho_\alpha \mathbf{U}_\alpha k_\alpha-\left(\mu+\frac{\mu_{T\alpha}}{\sigma_k}\right)\nabla k_\alpha\right)\right)\\&=r_\alpha S_{k\alpha}+\sum_{\beta=1}^{N_p} c_{\alpha\beta}^{(k)}\left(k_\beta-k_\alpha\right)\end{aligned} \tag{9}$$

$$\begin{aligned}&\nabla.\left(r_\alpha\left(\rho_\alpha \mathbf{U}_\alpha \varepsilon_\alpha-\left(\mu+\frac{\mu_{T\alpha}}{\sigma_\varepsilon}\right)\nabla \varepsilon_\alpha\right)\right)\\&=r_\alpha S_{\varepsilon\alpha}+\sum_{\beta=1}^{N_p} c_{\alpha\beta}^{(\varepsilon)}\left(\varepsilon_\beta-\varepsilon_\alpha\right)\end{aligned} \tag{10}$$

The source terms were considered to be the same as their single-phase analogous and thus:

$$S_{k\alpha}=P_\alpha-\rho_\alpha \varepsilon_\alpha \tag{11}$$

$$S_{\varepsilon\alpha}=\frac{\varepsilon_\alpha}{k_\alpha}\left(C_{1\varepsilon}P_\alpha-C_{2\varepsilon}\rho_\alpha \varepsilon_\alpha\right) \tag{12}$$

where P is the shear production.

The constants were set as

$C_\mu=0.09, C_1=1.44, C_2=1.92,$

$C_3=0, \sigma_k=1.00$ and $\sigma_\varepsilon=1.217$

Since air was considered as compressible flow, its density will then change with changes in pressure and temperature. The ideal gas law:

$$\rho=\frac{pW}{RT} \tag{13}$$

where $p=P+P_{ref}$

W, R, P and T denotes the molecular weight, universal gas constant, pressure and temperature respectively.

Geometry and Parameters

The cylindrical coordinate system was used to create the geometry for the conventional entrainment jet. The schematic diagram is shown in figure 1. The dimensions of the geometry and boundary conditions are shown in table 1. For three-phase flow (water, air and solid) the surrounding was considered to be in atmospheric condition. To take account of the surroundings extra blocks were created and atmospheric pressure boundary conditions were applied.

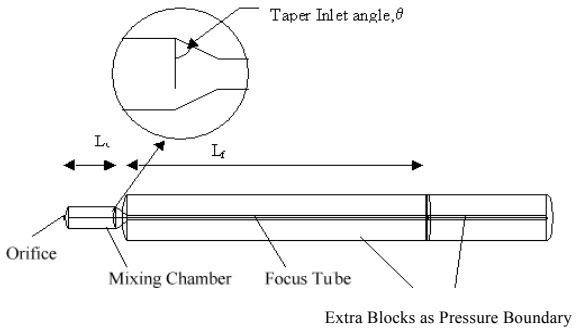

Figure 1. Schematic diagram of the AWJ nozzle

Nozzle dimension	
Orifice diameter	0.33 mm
Mixing chamber diameter	6 mm
Mixing chamber length, Lc	12 mm
Focus tube diameter, df	1.27 mm
Focus tube length, Lf	75 mm
Abrasive inlet diameter	3 mm
Water density	1000 kg/m3
Air density	1.29 kg/m3
Abrasive density	4100 kg/m3
Abrasive diameter	180 µm
Inlet conditions	
Water pressure	276 MPa
Air pressure	0.76 MPa
Abrasive mass flow rate	0.45 kg /min
Air flow rate	2.67 lit/min

Table 1. Geometry parameters and boundary conditions

Validation of the simulations

There are very few experiments done to find out the velocity distributions at the exit of the focus tube. In absence of the available experimental data, validation of the present numerical results were carried out by comparing with the experimental data for a two phase flow published by Zoltani and Bicen [11]. In their study a fully turbulent, two phase round jet of 25.4 mm diameter, with exit velocity of 20 m/s and containing 80 µm beads with a density of loading of 1.5% was examined. They used laser-Doppler Velocimetry to measure the velocity of air and solid for several positions at the exit. The results presented in figure 2 and 3 for air and solid show that the numerical simulations obtained are in good quantitative agreement with the experimental study. The speed ratio for water is shown in figure 4 showed the similar trend to that of air and solid (figure 2 and figure 3). Uom is the mean centre line velocity and Unom is the numerical centre line velocity.

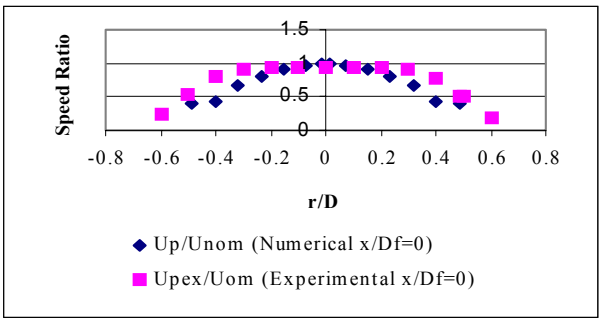

Figure 2. Speed ratio of the solid particles

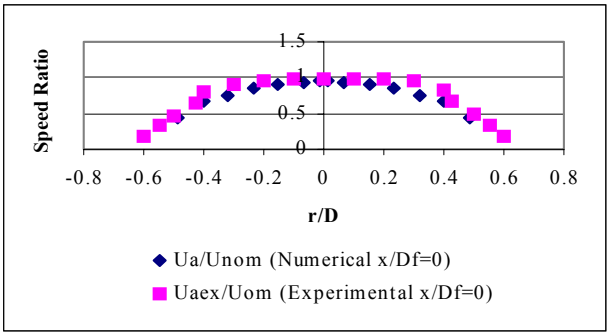

Figure 3. Speed ratio of air

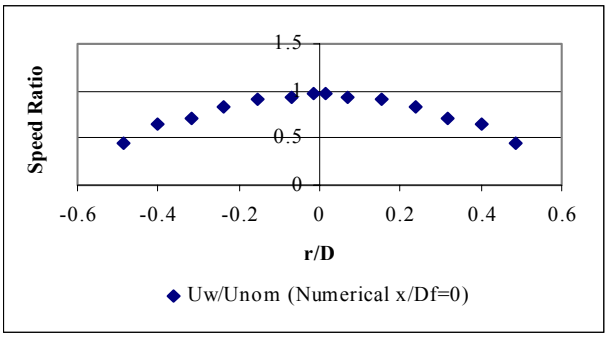

Figure 4. Speed ratio of water

The present numerical results are also validated against the measured experimental data of the volume fractions of the three phases. Neusen [5] measured the volume fraction of air, water and solid at the outlet using scanning X-ray densitometry, pressure ranging 207 to 345 MPa and abrasive flow rate from 0.34 to 0.57 kg/min. Measurement were taken at a stand-off distance of 4 mm. The air flow rate was not reported in their study. The comparisons are shown in figure 5 to figure 7. The discrepancy of the results are due to the air flow rate.

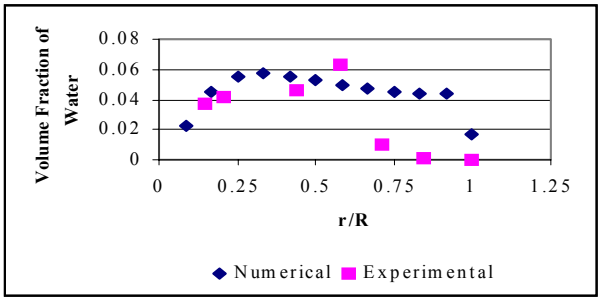

Figure 5. Volume Fraction of Water

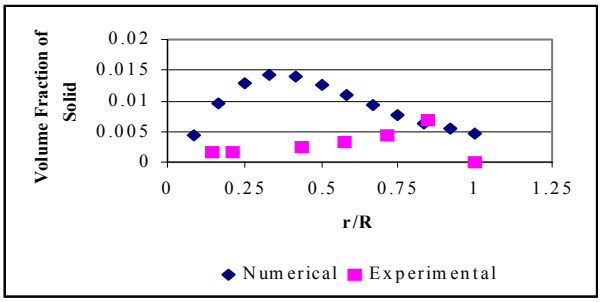

Figure 6. Volume Fraction of Solid

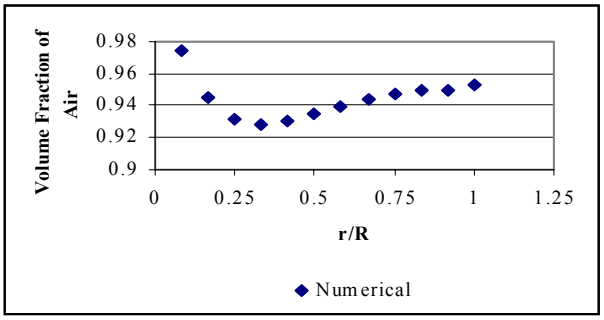

Figure 7. Volume Fraction of Air

Results and Discussions

The numerical simulations carried out to find out the effect of taper inlet angle in abrasive water jet are presented here in the form of velocities of different phases at the exit. Results presented in figure 8 and 9 clearly show that the taper inlet angle has influence on jet velocity at the exit of the focus tube. Andreas Momber [2] showed that a certain acceleration distance in the tapered region of the mixing chamber is necessary to accelerate the injected particles. When the taper inlet angle is small there are more collisions between the phases and the wall, in the tapered zone. So, at the smaller taper inlet angles the velocities at the outlet were low. In the case of larger taper inlet angles the particles are accelerated but with the increase of total travel length there are more chances of collisions with the wall. For precision cutting the jet velocity (all three phases) should be higher near the central axis region. Figure 8 shows the jet speed near the central axis for different taper inlet angles. The jet velocity (water, air and solid) for taper inlet angle of 60^0 is less than that for 45^0. But for the case of 75^0 the jet velocity increased again. It is clear from figure 8 that the relative speed of solid gradually increases with the increase of taper inlet angle. It is clear that there is a substantial influence of taper inlet angle on jet velocities. The average exit speed of the three phases are shown in figure 9 and it indicates that the jet speed reach a maximum at an optimum taper inlet angle of 75^0. The length of the tapered section of the mixing chamber is 8.8 mm at 75^0 and 27 mm at 85^0. This substantial increase in length results in more collision between the phases and also with the wall, leading to lower velocity at the exit at 85^0.

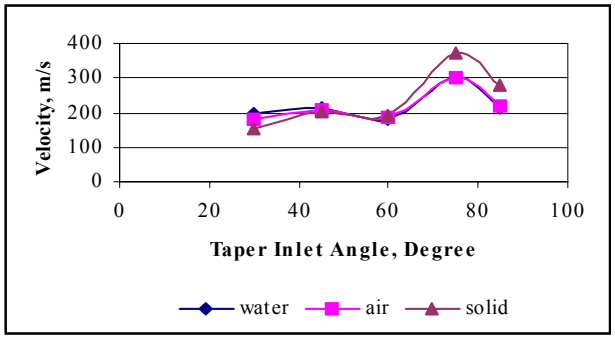

Figure 8. Velocities of different phases near the central axis for different taper inlet angle.

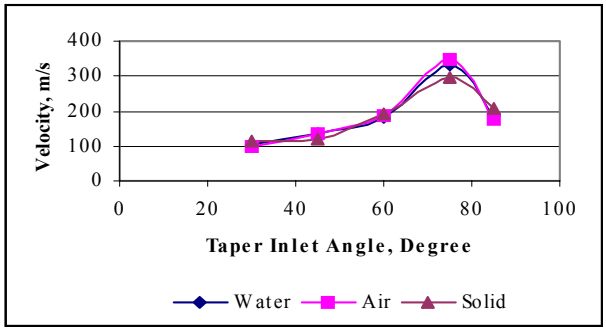

Figure 9. Average exit velocities of different phases for different taper inlet angle.

Conclusions

The following conclusions can be made from the results of the numerical simulation of abrasive water jet for different taper inlet angles.

- The jet velocity at the exit of the focus tube increases with the increase of taper inlet angle for up to 75^0.
- Beyond the taper inlet angle of 75^0, the jet velocity decreases. This may have been due to the fact that beyond 75^0, the length of the taper section becomes too long that leading to more collision and drag among the phases.
- The relative speed of solid gradually increases with the increase of taper inlet angle.
- Higher taper inlet angle at around 75^0 is necessary for the acceleration of the solid particles in abrasive water jet.

Acknowledgments

The authors would like to thank the Australian Research Council for the support of this project grant and well support of Industrial Research Institute Swinburne.

References

[1] Abduka, M., and Crofton, P. S. J., "Theoretical Analysis and Preliminary Experimental Result for an Abrasive Water Jet Cutting Head." *Proceedings of the 5th American Waterjet Conference*, 1989, Water Jet Technology Association, Toronto, Canada, pp 79-87.

[2] Andreas W. Momber and Radovan Kovacevic, "Principles of Abrasive Water Jet Machining". Springer Publisher. 1998, p. 212-215

[3] Hashish, M.: "Abrasive-fluid jet machining systems: entrainment versus direct pumping." *Jet Cutting Technology*, Essex, UK: Elsevier Science Publishers Ltd. 1991, pp 99-114

[4] Labus, T. J., Neusen, K. F., Albert, D. G., Gores, T. J., "Factors Influencing the Abrasive Mixing Process." *Proceedings of the 5th American Water Jet Conference,* 1989, Water Jet Technology Association, Toronto, Canada, pp 205-215.

[5] Neusen, K. F., Alberts, D. G., Gores, T. J., and Labus, T. J., "Distribution of Mass in a Three-Phase Abrasive Waterjet Using Scanning X-Ray Densitometry", *Proceedings 10th International Symposium on Jet Cutting Technology*, BHRG Fluid Engineering, Amsterdam, Netherlands, 1991, pp. 83-98.

[6] Neusen, K. F., Gores, T. J., and Amano, R. S., "Axial Variation of Particle and Drop Velocities Downstream From an Abrasive Water Jet Mixing Tube," *12th International Symposium on Jet Cutting Technology*, 1994, pp. 93-103.

[7] Scharner, M., Weseslindtner, H., Trieb, F., Herbig, N., and Haase, C., "Study on the Influence of Mixing Chamber Dimensions in Abrasive Waterjet Cutting Heads on Cutting Efficiency," *14th International Conference on Jetting Technology*, BHR Group Conference Series, Publication No. 32, 1998, pp. 169-183.

[8] Tazibt, A. Q., Parsy, F., and Abriak, N., "Theoretical Analysis of the Particle Acceleration Process in Abrasive Water Jet Cutting," *Computational Material Science*, Vol. 5, 1996, pp. 243-254.

[9] Ye, J., "Numerical Simulation of Particle Concentration at the Exit of a Direct Injected Abrasive Water Jet Nozzle," Particulate Science and Technology, Vol. 14, 1996, pp.75-88.

[10] Ye, J., and Kovacevic, R., "Turbulent Solid-Liquid Flow Through the Nozzle of Premixed Abrasive Water Jet Cutting System," *Proc. Instn Mech Engineers*, Vol.213, Part B, 1999, pp. 59-67.

[11] Zoltani, C. K., and Bicen, A. F., "Velocity Measurement in a Turbulent, Dilute, Two-phase Jet," Experiments in Fluids, Vol. 9, 1990, pp. 295-300.